

# The Combined Effect of Current Boosting and Power Loss on Photovoltaic Arrays under Partial Shading Conditions

Abdullahi Abubakar Mas'ud

Department of Electrical Engineering, Jubail Industrial College, Saudi Arabia  
masud\_a@rcjy.edu.sa  
(corresponding author)

Received: 24 September 2022 | Revised: 23 October 2022 | Accepted: 25 October 2022

## ABSTRACT

This study proposes a novel technique for improving the performance of photovoltaic (PV) arrays under Partial Shading Conditions (PSCs). A 4x4 solar PV array with 16 panels was considered. Bridge-Linked (BL), Total Cross-Tied (TCT), Honey Comp (HC), One Cross-Link (OCL), and Two Cross-Link (TCL) were among the topologies of interest. First, the combined effect of connecting switches and partial shading on the PV array was studied. Then, the power loss/gain caused by reconfiguring the PV array structure from Series-Parallel (SP) to other schemes was investigated. Finally, a method of boosting current into the PV array is proposed to reduce PSCs-related power losses in the connecting switches. The results show that the number of connecting switches in the topology plays an important role in determining power gain or loss at different partial shading levels. TCT and HC outperformed the others in terms of power improvement when PSCs were considered without current boosting. This is true for different levels of solar irradiation exposure. The SP topology is optimal when the solar irradiation level is greater than 900W/m<sup>2</sup> or less than 200W/m<sup>2</sup>. TCT outperformed the others when the current was boosted in the PV array, with a power improvement of 108%, for certain PSCs.

*Keywords-partial shading conditions; photovoltaic; total cross-tied; bridge coupled; honeycomb*

## I. INTRODUCTION

It is widely accepted that the global electricity demand is increasing rapidly, but the amount of fossil fuels available for power production is limited [1, 2]. On the other hand, fossil fuel emissions contribute to environmental pollution [3, 4]. As a result, renewable energy sources for power generation are widely advocated. Among these, solar photovoltaic (PV) technology has advanced significantly during the recent years [5, 6]. So far, it is one of the most imaginative developments, with the highest probability of dominating the Renewable Energy (RE) market [7]. Because of their low maintenance, zero pollution, and low-noise characteristics, PV systems have a wide range of applications, including solar vehicles, streetlights, and other hybrid energy systems [8, 9]. On the other hand, the output characteristics of PV panels are primarily determined by temperature and irradiance, and they are frequently unpredictable [9, 11]. When PV modules experience partial shading, they are not exposed to the same amount of irradiance. This results in inconsistent module characteristics [11]. Partial Shading Conditions (PSCs) occur when some modules in a PV array are shaded by trees and buildings and this results in the reduction of the voltage and current of the afflicted panel [12-15]. The panel that generates the least amount of electricity will act as an electrical load drawing energy from the system's other modules [14, 15],

resulting in a decrease in the overall power output. Partial shading can be reduced by selecting appropriate PV topologies or physically reconfiguring PV modules, as well as employing Maximum Power Point Tracking (MPPT) technologies. The most common configurations for PV arrays are honeycomb (HC), Series-Parallel (SP), Total Cross-Tied (TCT), and Bridge-Link (BL) [20-21]. Under various PSCs, the TCT has the lowest mismatch losses and the highest power output. In [20], it has been shown that the TCT configuration does not deliver the maximum power possible when operating in partial shading and the extracted output power can be further increased [20].

Several researchers have investigated different techniques to reduce mismatching power losses in PV arrays [5, 17, 23-33]. Authors in [27] compared large interconnected SP array schemes operating under PSCs [27]. These combinations were modeled and analyzed in MATLAB/Simulink, and the results were validated experimentally. The result indicates that the Global Maximum Power point (GMPP) depends on the shading pattern and the architecture of the PV array. Authors in [22] developed a modified bypass circuit that effectively finds a compromise between the increased reliability and the increased complexity of the PV array. The results were validated experimentally. The bypass circuit worked well in lowering the hot spot temperature of the cryptic cell below the average

temperature of the module without significantly increasing the complexity of the system. Genetic Algorithm [33], Particle Swarm Optimization [34], Mine Blast Optimization [35], Cuckoo Search [36], and Ant Colony Optimization [34] are other examples of optimization techniques deployed for minimizing losses under PSCs.

Recently, authors in [23] proposed an improved technique to enhance the performance of the PV array technologies (PVAT) under PSCs. The study takes into account 8 shading patterns. To combat partial shading, 6 novel PVATs based on specific array configurations were presented. The simulation results were compared to those obtained with conventional PVATs, and the best topologies for different PSCs are determined. The TCT typically achieves maximum power extraction from PSCs. It also enhanced PVAT output power for short and wide PSC by 105%. The performance of the TCT was enhanced in another investigation employing the minimizing losses technique [25]. Different arrangements were introduced by reducing the number of connecting switches. The PV module configuration was altered to generate 5% more power in PSCs. If 50% or more of the area was partially shadowed, no reconfiguration was required. When the darkened region was less than 50%, reconfiguration significantly increased power.

Many studies have developed PV reconfiguration strategies that can reduce the impact of PSCs on PV arrays. However, one aspect that has yet to be investigated is the way PV arrays perform under PSCs, when both current boosting and switch losses are considered. A PV array reconfiguration, on the other hand, necessitates an increase in the number of switches, resulting in increased switching power loss and the need for more current to be boosted during PSCs. Therefore, in this paper, a novel strategy for minimizing losses in PV arrays under PSCs is presented. The approach involves boosting the current in the partially shaded sections of the PV array. To obtain a more robust result, current losses in connecting switches are also considered. A 4x4 PV array with 4 shading patterns was investigated, and all simulations were performed in MATLAB/SIMULINK. Configurations of interest include SP, TCT, HC, BL, OCL, and TCL.

II. MATERIALS AND METHODS

A. Modeling of the PV Array

The PV cell is the most important part of a PV system because it converts energy from the sun to electricity [38, 40]. The amount of electricity produced by a PV module or cell is primarily determined by temperature and solar irradiation. Because of its higher accuracy in obtaining the shunt and series resistances, the single diode model of a PV cell has been used in PV modeling [28, 42]. A PV module is a grouping of PV cells connected in series, whereas a PV array is a grouping of PV modules connected in series or parallel, as well as a slew of others [21, 43]. Equation (1) depicts the mathematical representation of the current-voltage (I-V) characteristics for an ideal PV cell model with a terminal current [29].

$$I = I_{PV} - I_0 \left[ \exp \left( \frac{q(V + R_S)}{A k_B T} \right) - 1 \right] - \frac{V + R_{SH}}{R_{SH}} \tag{1}$$

where  $I_0$  represents the saturation current of the diode,  $I_{PV}$  represents the current of the PV,  $V$  represents the PV module's terminal voltage,  $A$  represents the ideality factor,  $k_B$  is the Boltzmann's constant,  $q$  represents the electronic charge,  $R_S$  represents the series resistance,  $T$  represents the junction temperature, and  $R_{SH}$  represents the shunt resistance.

The 4x4 PV module is designed in MATLAB/SIMULINK using a single diode PV model. Equation (2) describes the I-V characteristics of a PV array composed of  $N_p$  parallel and  $N_s$  series-connected modules [41].

$$I = I_{PV} N_p - I_r N_p \left[ \exp \left( \frac{q \left( V + R_S \frac{N_s}{N_p} \right) I}{A k_B T} \right) - 1 \right] - \frac{V + R_S \frac{N_s}{N_p}}{R_{SH} \frac{N_s}{N_p}} \tag{2}$$

where  $I$  represents the diode reverse leakage current. The parameters of the 25W Blue solar PV module that was used to model the PV array schemes are listed in Table I.

TABLE I. PARAMETERS FOR THE 25W SOLAR PV MODULE

S/No	Parameters	Values
1	Maximum power of the PV	25W
2	Short circuit current of the PV ( $I_{sc}$ )	1.45A
3	Open circuit voltage of the PV ( $V_{oc}$ )	22.2V
4	Current at the maximum power	1.37A
5	The voltage at the maximum power	18.2V
6	The temperature coefficient of $V_{oc}$	-0.34%/°C
7	Cells per module	40
8	Cells per module	40
9	Temperature coefficient of $I_{sc}$	0.041%/°C
10	$R_{SH}$	1114.063Ω
11	$R_S$	0.9635Ω

B. Proposed PV Module Configuration

To reduce the partial shading impact, PV array arrangement is critical. A proper array arrangement must be adopted to produce the necessary power output improvement from the PV array system. Some of the most commonly used PV array configurations in the literature are SP, TCT, BL, and HC [42]. Among them, the SP (see Figure 1(a)) is the most widely used. Under the PSCs, the SP scheme is the most effective against mismatch power losses in series strings. To minimize mismatch power losses in series strings, alternative tie connections are inserted between the parallel strings of a SP scheme. They are designed in the BL, HC, and TCT configurations. Figure 1(b) is the BL scheme. The PV modules resemble a bridge rectifier arrangement. One drawback of the BL arrangement is that it performs poorly under PSCs. The TCT configuration is shown in Figure 1(d). To design the TCT arrangement, cross ties must be connected between each module in the SP scheme. These cross-links connect the modules in the array arrangement.

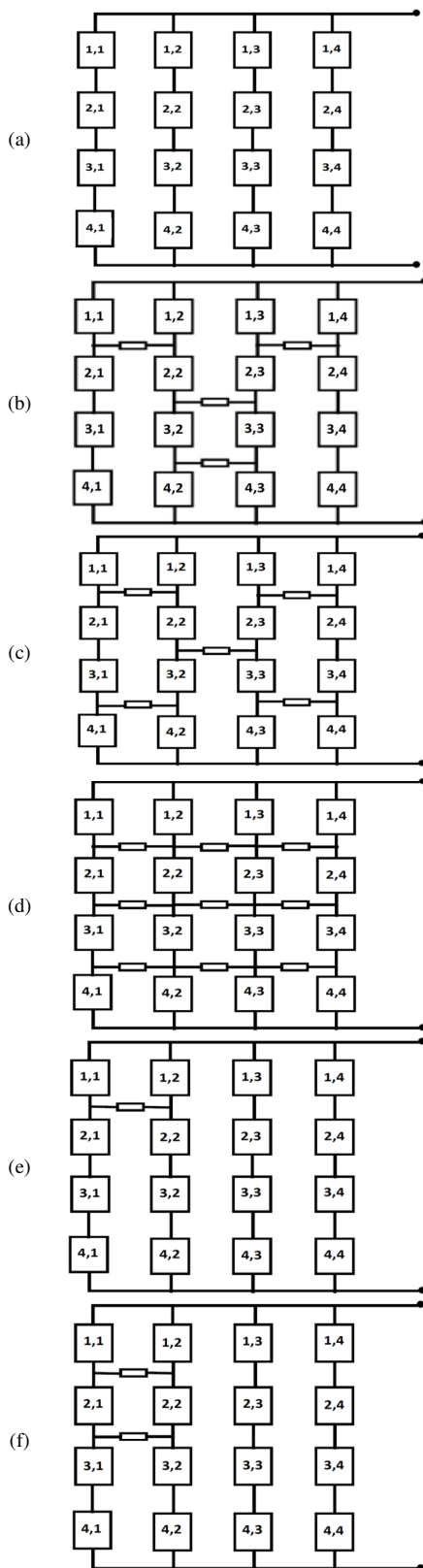


Fig. 1. PV array schemes considered: (a) BP, (b) BL, (c) HC, (d) TCT, (e) OCL, (f) TCL.

The cross ties help reduce mismatch losses in the shaded module's series string by providing an additional current channel. TCT, on the other hand, suffers from high initial installation costs and cable losses due to the extensive interconnections. To reduce these losses, some interconnections can be disabled and set to either HC or BL. In this study, two additional schemes will be considered, i.e. one and two crosslinks in the SP configurations (see Figure 1(e)-(f)). Previous research did not consider non-ideal switches between crosslinks, particularly during PV shading mitigation using the current boosting method [23]. Due to the fact that these switches can result in additional power losses during PSCs, the purpose of this study is to examine the possibility of incorporating crosslink switching into the current boosting procedure. In this instance, a more reliable result will be obtained.

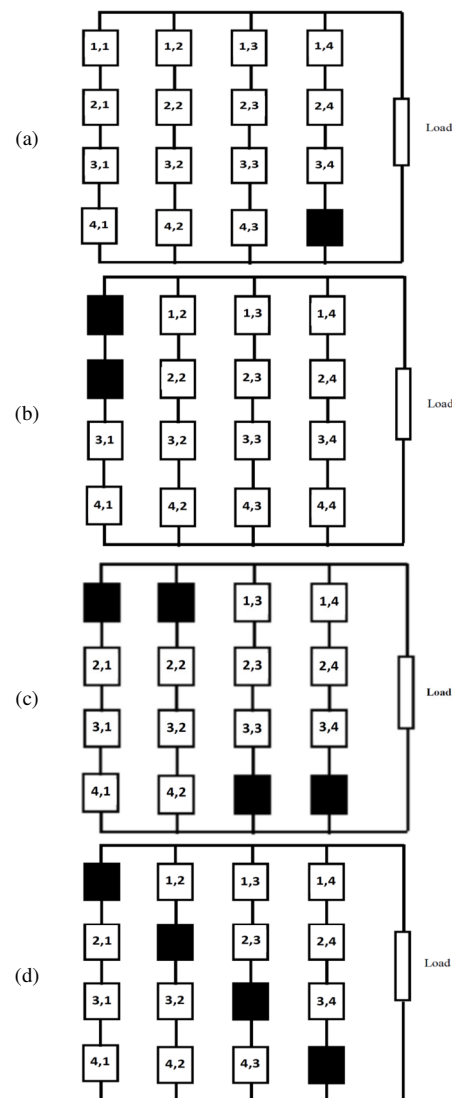


Fig. 2. Shading patterns on the PV scheme. Cases (a) 1, (b) 2, (c) 3 (d) 4.

C. Proposed Partial Shading Schemes

When PSCs occur, portions of the PV array will not receive the required level of irradiance. As a result, the shading scenario is unpredictable. As shown in Figure 2, four shading conditions will be considered to analyze the partial shading effect on the 4x4 PV modules:

- Case 1: A single PV module is shaded.
- Case 2: Two PV modules are shaded.
- Case 3: Four PV modules are shaded
- Case 4: Four PV modules are shaded (diagonally).

As previously stated, this study investigates the effects of shading on PV modules at 40°C with varying amounts of irradiance. Under the same conditions, when the PV array is uniformly shaded, the irradiance value of all 16 modules is exactly 1000W/m<sup>2</sup>. Solar radiation reduction from 900W/m<sup>2</sup> to 100W/m<sup>2</sup> will be considered for all PSCs. Each model ran with a load of 13.2Ω.

III. CURRENT BOOSTING PROCEDURE

A current boosting strategy has been proposed in [14] which improves PV power during PSCs. However, the current boosting procedure for different schemes has not been well investigated. A more in-depth analysis will be provided in this study. In this study, the current is directly boosted across the partially shaded panel, with a bypass diode connected across all PV modules to provide a low resistance path for the flow of any current, thereby improving the GMPP. Although using bypass diodes increases the cost and complexity of any PV array, it can significantly improve power during PSCs. Previous research has shown that under PSCs and with bypass diodes, the GMPP for SP, TCT, HC, and BL PV topologies is 21.54%, 52.74%, 16.09%, and 20.78% higher than what it would be in a scheme without bypass diodes [32]. The bypass diodes across a PV panel can cause peaks in the P-V characteristic curve but are not detrimental to the system.

In this study, the bypass diode was utilized. Figure 3 depicts the current boosting schemes for each of the considered topologies. Equation (3) is a generalized equation that shows the current produced by a PV module in a TCT architecture [14].

$$I_{ni} = \frac{G_{ni}}{G_{STC}} \times I_g, \quad 1 < i < d \tag{3}$$

where  $n$  denotes the number of rows and  $d$  the number of PV panels.  $G_{STC}$  denotes irradiation at standard temperature conditions, whereas  $G_{ni}$  denotes irradiation received by a PV panel.  $I_g$  denotes the maximum current generated by a PV panel under STCs. The total current generated in each row is the sum of the currents generated in each PV module in that row. The mismatch current in the TCT topology is the difference between the total current under PSCs and the peak value of the current without PSCs. The mismatch current will be boosted across the specific row to improve power during the current boosting procedure. The current is boosted across the shaded rows on the TCT topology at every instant, based on the partial

shading situation, as shown in Figure 3. The boosted current scheme cannot be implemented in the other topologies shown in Figure 3 (BL, HC, OCL, and TCL). In this case, regardless of the shaded PV panel in the topology, the current will only be boosted at specific locations. This is proposed to comply with circuit theory rules and to avoid boosting current in places where it is not required. Because there are fewer interlink connections between neighboring strings in these topologies than in the conventional TCT topology, mismatch losses are greater. However, the proposed scheme will only provide the best PV or I-V characteristic curve in TCT configuration.

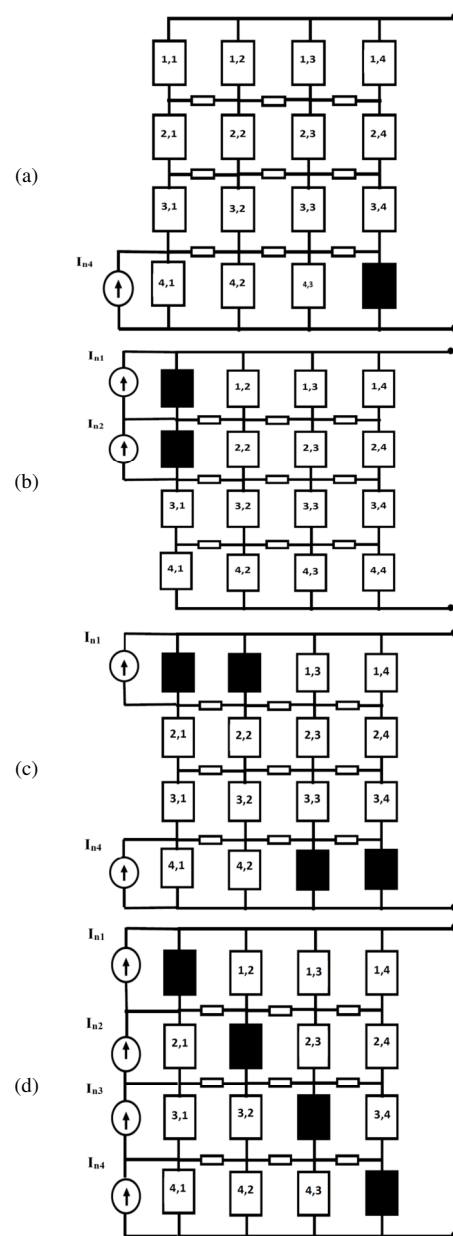


Fig. 3. Current boosting scheme for a TCT configuration under PSCs.

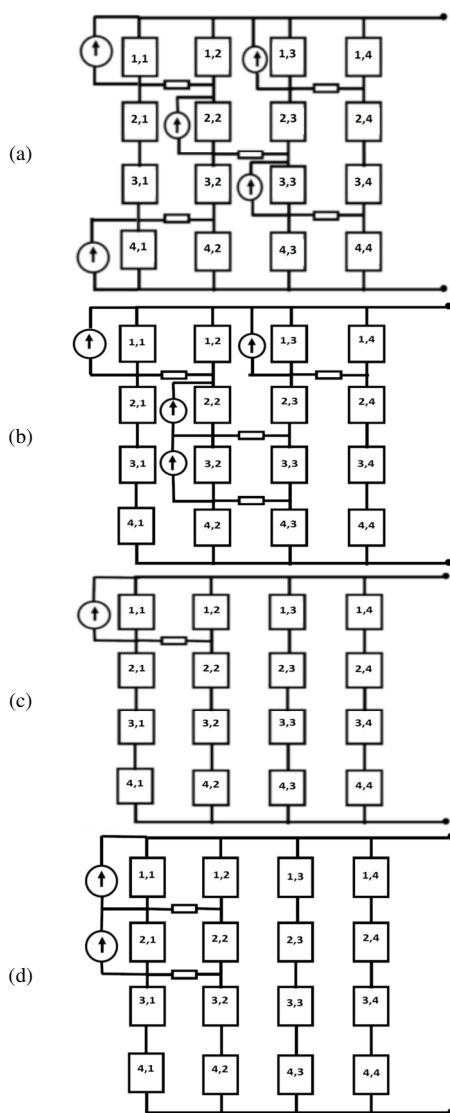


Fig. 4. Current boosting schemes with connecting switches under PSCs: (a) HC, (b) BL, (c) OCL, (d) TCL.

IV. RESULT AND DISCUSSIONS

MATLAB/Simulink was utilized to simulate a 4x4 PV array with 5 different configurations (i.e. SP, BL, HC, TCT, OCL, and TCL) and 4 different shading patterns (cases 1-4). First, the combined effect of connecting switches and partial shading on the power output of 5 PV topologies (BL, HC, TCT, OCL, and TCL) was investigated. Then, the power loss/gain caused by switching from SP to the aforementioned topologies was investigated. A current boosting technique was subsequently used to see if the performance of the PV array had improved. The ultimate goal was to use as few switches as possible in order to minimize switch loss. When partial shading occurs, this approach may be able to produce the best architecture in terms of peak output power. Table II shows a comparison of the proposed and existing PV topologies under 4 distinct PSCs. In contrast to the current topology, the proposed method employs the boosting current strategy.

TABLE II. THE OUTPUT POWER IMPROVEMENT OF ALL SCHEMES UNDER VARIOUS PSCS

Switch combinations	PV shading configuration	$G_{MPP}(W)$		Total boosted current (A)	Power Improvement (W)
		Existing scheme	Proposed scheme		
All switches closed (TCT)	Case 1	266.72	350.21	0.79	84.49
	Case 2	263.9	344.13	1.64	80.23
	Case 3	132.11	370.2	5.528	228.09
	Case 4	259.13	337.32	3.4	78.19
Switches 1,3,5,7,9 closed (HC)	Case 1	266.44	344.45	0.748	78.01
	Case 2	262.50	337.88	1.562	75.38
	Case 3	139.23	362.0	5	223
	Case 4	261.33	335	3.164	73.67
Switches 1,5,6,7 closed (BL)	Case 1	265.99	336.4	0.75	70.41
	Case 2	263.53	337.60	1.6	74.07
	Case 3	208.57	356.70	4.432	148.13
	Case 4	219.76	323	3.68	103.24
Switches 1,2 closed (OCL)	Case 1	274.65	330.33	0.69	55.68
	Case 2	264.87	340.989	0.77	76.12
	Case 3	228.20	326.50	1.1	98.3
	Case 4	212.32	360.17	1.254	147.85
Switch 1 closed (TCL)	Case 1	275.11	328.39	0.66	53.28
	Case 2	263.91	338.49	0.79	74.6
	Case 3	228.75	321.93	1.09	93.18
	Case 4	212.611	357.77	1.16	145.16

First, the shaded PV module is assumed to have a solar irradiation level of  $100W/m^2$ , implying very low PV shading. When one of the 16 PV panels is shaded, the HC, TCT, and BL configurations suffer more losses than the others, with the TCL arrangement appearing to be the most efficient because the shaded PV module is at the end of the topology and the TCT has more interconnecting switches than the OCL and TCL. Furthermore, in Case 1, the more connecting switches there are, the greater the power loss. For Case 2, the power loss under PSCs appears to be nearly identical for all topologies, with TCL appearing to be the optimum. Because the shaded panels are in the upper left quadrant of the array, close to the two connecting switches, current may flow in a different direction during partial shading. Case 3 appears to favor OCL and TCL, though BL outperforms TCT and HC. This is an indication that the number of connecting switches increased the power loss of the complete system. This conclusion, however, does not apply to all PV shading situations. The TCT and HC appear to perform best in Case 4, where the shading appears in a diagonal form, demonstrating that the scheme's performance improves with more connecting switches. In general, it appears that the shading pattern in Case 3 causes more power loss than the others.

Figures 5–8 show the percentage of power loss or gain when converting from SP to HC, BL, TCT, OCL, and TCL configurations. Solar radiation is varied between  $900$  and  $100W/m^2$ , and each shading pattern is investigated. It should be noted that the percentage of power loss/gain for BP is zero in all the Figures because it was assumed to be the reference configuration. TCT is the best configuration when switching from BP to the others in Case 1 (Figure 5), followed by HC. At  $500W/m^2$ , TCT and HC improve power by 3% and 1.8%, respectively.

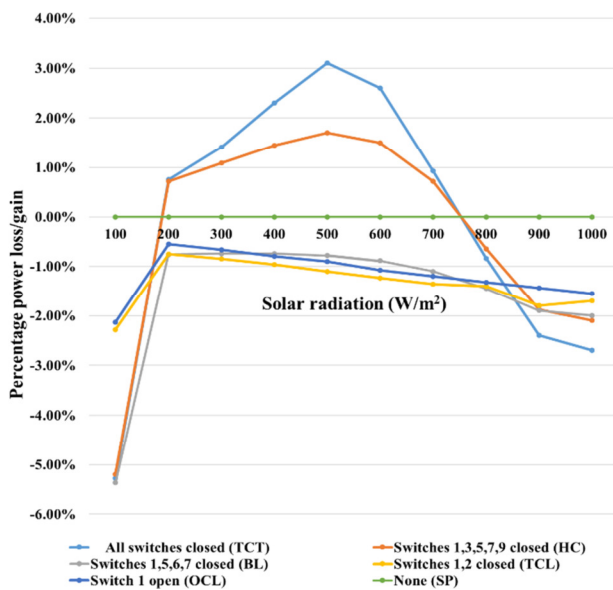


Fig. 5. The percentage of power loss/gain when switching from SP to the other configurations in Case 1.

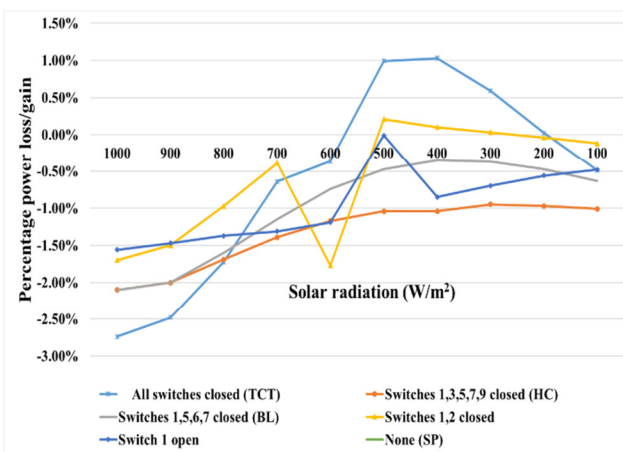


Fig. 6. The percentage of power loss/gain when switching from SP to the other configurations in Case 2.

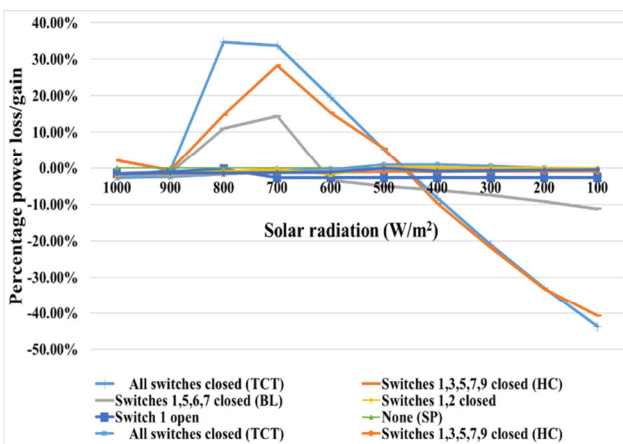


Fig. 7. The percentage of power loss/gain when switching from SP to the other configurations in Case 3.

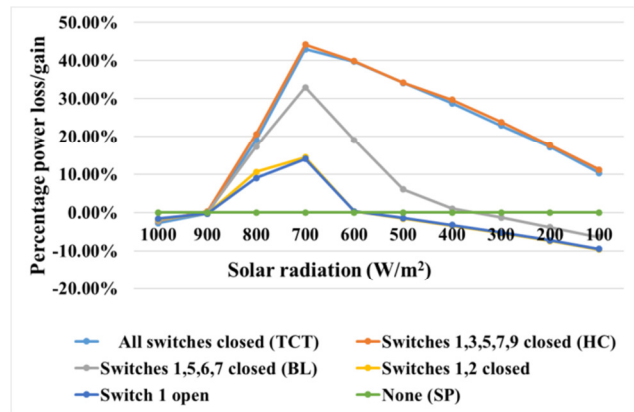


Fig. 8. The percentage of power loss/gain when switching from SP to the other configurations in Case 4.

The solar radiation in the shaded module for Case 1 should be between 200 and 700W/m<sup>2</sup> for any power improvement in the TCT and HC. TCT is the best configuration for Case 2 (Figure 6), followed by TCL. Power improvements of 1% have been made. In Case 3 (Figure 7), when reconfiguring from BP to TCT, the TCT appears to outperform the others. In this case, however, the HC performs nearly as well as the TCT. This performance is only noticeable when the solar radiation on the shaded module exceeds 500W/m<sup>2</sup>. However, reconfiguration from BP to the other schemes below 500W/m<sup>2</sup> results in a power loss of up to 50% for TCT and HC and 10% for the BL. As a result, when reconfiguring PV modules under PSCs, care must be taken because significant power losses are possible and thus detrimental at certain solar irradiation levels. In Case 4, the TCL and HC appear to outperform the others at nearly all irradiation levels. As a result, it appears that this is an appropriate scheme for this type of partial shading. It is important to note that the TCT can achieve maximum power improvements of 3%, 1%, 35%, and 42% for Case 1, Case 2, Case 3, and Case 4 shading configurations, respectively.

When the boosted current values in Table II are examined, it is clear that the TCT receives more boosted current than the others for all of the PV shading schemes considered. This is because a current is boosted in every row with mismatching power in the TCT, whereas in the other cases, a current is boosted in specific rows regardless of shading location. Despite the fact that the GMPP value will improve, one major disadvantage of non-uniform current boosting is the formation of numerous peaks in the characteristic curves. TCT appears to be the best strategy in terms of power improvement when considering the proposed technique (see Figure 9). Case 3 shading pattern can improve power by up to 228W. The TCT has more interconnecting switches than the others, and the mismatch current is enhanced in each row. Figure 9 shows the proposed and existing P-V and I-V curves for TCT in each of the 4 partial shading scenarios. The P-V curve of the proposed technique has fewer peaks than the existing technique, with power improvements of 31%, 30%, 108%, and 30.1% for Case 1, Case 2, Case 3, and Case 4, respectively. For Cases 3 and 4, the proposed technique has one peak, whereas the existing technique has two peaks.

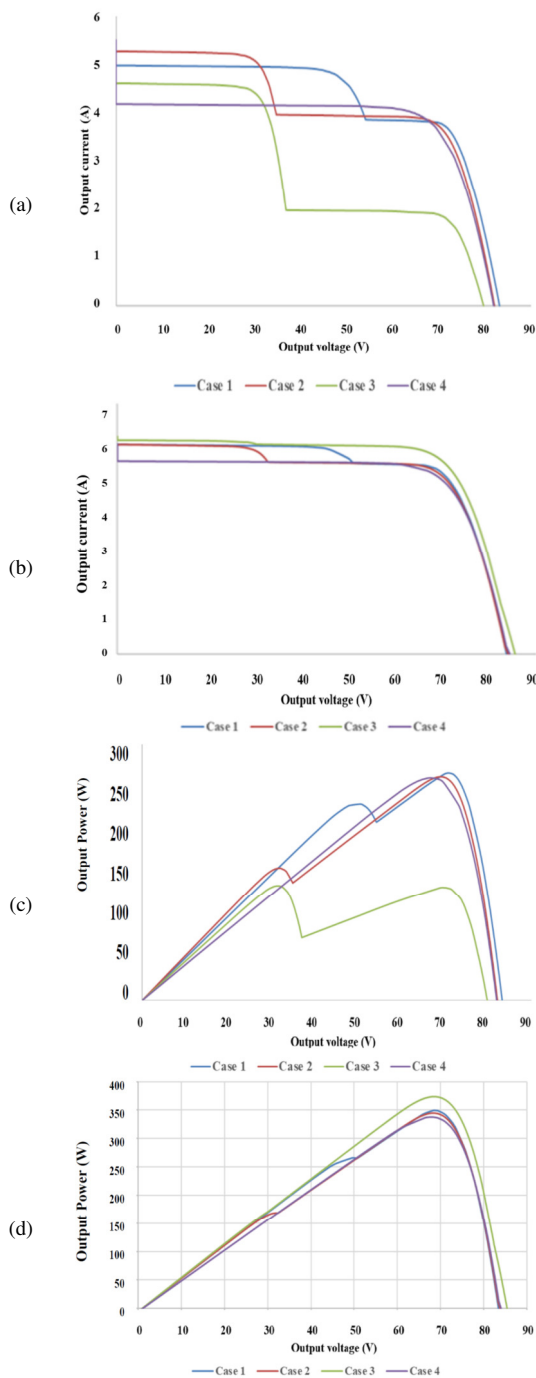


Fig. 9. I-V curve of the (a) existing PV scheme, (b) proposed TCT scheme. P-V curve of the (c) existing PV scheme, (d) proposed P-V scheme.

Despite a significant power improvement, the number of peaks in Cases 1 and 2 is the same for both the existing and proposed techniques. In this study, the P-V and I-V curves for the other switching configurations (BL, HC, OCL, and TCL) were not shown, because the number of peaks does not change even with current boosting, and only power improvement is visible. The current boosting scheme, as described in the literature, cannot be implemented in the SP configuration [14].

According to the results of this study, reconfiguration of the BP scheme under PSCs may not be required for certain solar irradiation levels. Furthermore, current boosting will result in power gains relative to any of the commonly used PV topologies, i.e. TCT, HC, BL, OCL, and TCT, and the power loss in the connecting switches plays a significant role in the amount of current boosted during PSCs.

## V. CONCLUSION

In this study, the effect of current boosting and power loss caused by connecting switches on the I-V and P-V characteristic curves of a PV array were investigated. MATLAB/Simulink was utilized to simulate 4x4 PV array under various degrees of shade and shading patterns. The shading patterns of 4, 2, and 1 in 16 PV panels were investigated. Power loss or gain as a result of reconfiguring PV panels from the BP to other configurations such as BL, TCT, HC, OCL, and TCL has been studied in depth. The level of solar irradiation at which the PV array could be reconfigured was also evaluated. The results show that the number of connecting switches in the topology is an important factor in determining power gain/loss at various shading levels. The more connecting switches there are, the more power is lost, and more current is required to compensate for the power mismatch. TCT and HC appear to outperform the others in terms of power improvement for the majority of the partial shading scenarios considered without current boosting. This is only true for certain solar irradiation levels. It has also been shown that, under certain shading patterns (case 4, diagonal shading), up to 50% of the power is lost when compared to the BP scheme. In the case of current boosting, TCT showed greater power improvement than others because, in TCT, current is boosted in every row with power mismatch, whereas in the other cases, current is boosted in specific rows regardless of the shading position. For a specific shading pattern, the proposed technique improved power by up to 108%. The results show that for the majority of the shading patterns considered, the BP scheme is the best for solar irradiation level higher than  $900\text{W/m}^2$  or lower than  $200\text{W/m}^2$ .

## ACKNOWLEDGMENT

The author wishes to acknowledge the support given by Jubail Industrial College during this research.

## REFERENCES

- [1] K. Chen, S. Tian, Y. Cheng, and L. Bai, "An Improved MPPT Controller for Photovoltaic System Under Partial Shading Condition," *IEEE Transactions on Sustainable Energy*, vol. 5, no. 3, pp. 978–985, Jul. 2014, <https://doi.org/10.1109/TSTE.2014.2315653>.
- [2] D. K. Dhaked, Y. Gopal, and D. Birla, "Battery Charging Optimization of Solar Energy based Telecom Sites in India," *Engineering, Technology & Applied Science Research*, vol. 9, no. 6, pp. 5041–5046, Dec. 2019, <https://doi.org/10.48084/etasr.3121>.
- [3] J. Ma, D. Hong, K. Wang, Z. Bi, X. Zhu, and J. Zhang, "Analytical modeling and parameter estimation of photovoltaic strings under partial shading conditions," *Solar Energy Materials and Solar Cells*, vol. 235, Jan. 2022, Art. no. 111494, <https://doi.org/10.1016/j.solmat.2021.111494>.
- [4] O. Bingöl and B. Özkaya, "Analysis and comparison of different PV array configurations under partial shading conditions," *Solar Energy*, vol. 160, pp. 336–343, Jan. 2018, <https://doi.org/10.1016/j.solener.2017.12.004>.

- [5] N. Belhaouas *et al.*, "A new approach of PV system structure to enhance performance of PV generator under partial shading effect," *Journal of Cleaner Production*, vol. 317, Oct. 2021, Art. no. 128349, <https://doi.org/10.1016/j.jclepro.2021.128349>.
- [6] D. K. Dhaked and D. Birla, "Microgrid Designing for Electrical Two-Wheeler Charging Station Supported by Solar PV and Fuel Cell," *Indian Journal of Science and Technology*, vol. 14, no. 30, pp. 2517–2525, Sep. 2021, <https://doi.org/10.17485/IJST/v14i30.224>.
- [7] D. K. Dhaked and D. Birla, "Modeling and control of a solar-thermal dish-stirling coupled PMDC generator and battery based DC microgrid in the framework of the ENERGY NEXUS," *Energy Nexus*, vol. 5, Mar. 2022, Art. no. 100048, <https://doi.org/10.1016/j.nexus.2022.100048>.
- [8] H. Rezk, I. Tyukhov, and A. Raupov, "Experimental implementation of meteorological data and photovoltaic solar radiation monitoring system," *International Transactions on Electrical Energy Systems*, vol. 25, no. 12, pp. 3573–3585, 2015, <https://doi.org/10.1002/etep.2053>.
- [9] H. Rezk, I. Tyukhov, M. Al-Dhaifallah, and A. Tikhonov, "Performance of data acquisition system for monitoring PV system parameters," *Measurement*, vol. 104, pp. 204–211, Jul. 2017, <https://doi.org/10.1016/j.measurement.2017.02.050>.
- [10] M. H. Zafar *et al.*, "Group Teaching Optimization Algorithm Based MPPT Control of PV Systems under Partial Shading and Complex Partial Shading," *Electronics*, vol. 9, no. 11, Nov. 2020, Art. no. 1962, <https://doi.org/10.3390/electronics9111962>.
- [11] G. Sai Krishna and T. Moger, "Improved SuDoKu reconfiguration technique for total-cross-tied PV array to enhance maximum power under partial shading conditions," *Renewable and Sustainable Energy Reviews*, vol. 109, pp. 333–348, Jul. 2019, <https://doi.org/10.1016/j.rser.2019.04.037>.
- [12] Y. Kassem, H. Camur, and O. a. M. Abughinda, "Solar Energy Potential and Feasibility Study of a 10MW Grid-connected Solar Plant in Libya," *Engineering, Technology & Applied Science Research*, vol. 10, no. 4, pp. 5358–5366, Aug. 2020, <https://doi.org/10.48084/etasr.3607>.
- [13] F. Belhachat and C. Larbes, "PV array reconfiguration techniques for maximum power optimization under partial shading conditions: A review," *Solar Energy*, vol. 230, pp. 558–582, Dec. 2021, <https://doi.org/10.1016/j.solener.2021.09.089>.
- [14] J. Ahmed and Z. Salam, "A critical evaluation on maximum power point tracking methods for partial shading in PV systems," *Renewable and Sustainable Energy Reviews*, vol. 47, pp. 933–953, Jul. 2015, <https://doi.org/10.1016/j.rser.2015.03.080>.
- [15] N. Priyadarshi *et al.*, "Performance Evaluation of Solar-PV-Based Non-Isolated Switched-Inductor and Switched-Capacitor High-Step-Up Cuk Converter," *Electronics*, vol. 11, no. 9, Jan. 2022, Art. no. 1381, <https://doi.org/10.3390/electronics11091381>.
- [16] R. K. Pachauri *et al.*, "Impact of Partial Shading on Various PV Array Configurations and Different Modeling Approaches: A Comprehensive Review," *IEEE Access*, vol. 8, pp. 181375–181403, 2020, <https://doi.org/10.1109/ACCESS.2020.3028473>.
- [17] B. Yang *et al.*, "Comprehensive overview of maximum power point tracking algorithms of PV systems under partial shading condition," *Journal of Cleaner Production*, vol. 268, Sep. 2020, Art. no. 121983, <https://doi.org/10.1016/j.jclepro.2020.121983>.
- [18] H. Braun *et al.*, "Topology reconfiguration for optimization of photovoltaic array output," *Sustainable Energy, Grids and Networks*, vol. 6, pp. 58–69, Jun. 2016, <https://doi.org/10.1016/j.segan.2016.01.003>.
- [19] G. Sai Krishna and T. Moger, "Reconfiguration strategies for reducing partial shading effects in photovoltaic arrays: State of the art," *Solar Energy*, vol. 182, pp. 429–452, Apr. 2019, <https://doi.org/10.1016/j.solener.2019.02.057>.
- [20] F. Belhachat and C. Larbes, "Modeling, analysis and comparison of solar photovoltaic array configurations under partial shading conditions," *Solar Energy*, vol. 120, pp. 399–418, Oct. 2015, <https://doi.org/10.1016/j.solener.2015.07.039>.
- [21] S. Sugumar, D. Prince Winston, and M. Pravin, "A novel on-time partial shading detection technique for electrical reconfiguration in solar PV system," *Solar Energy*, vol. 225, pp. 1009–1025, Sep. 2021, <https://doi.org/10.1016/j.solener.2021.07.069>.
- [22] S. Ghosh, V. K. Yadav, and V. Mukherjee, "Improvement of partial shading resilience of PV array through modified bypass arrangement," *Renewable Energy*, vol. 143, pp. 1079–1093, Dec. 2019, <https://doi.org/10.1016/j.renene.2019.05.062>.
- [23] D. Prince Winston, S. Kumaravel, B. Praveen Kumar, and S. Devakirubakaran, "Performance improvement of solar PV array topologies during various partial shading conditions," *Solar Energy*, vol. 196, pp. 228–242, Jan. 2020, <https://doi.org/10.1016/j.solener.2019.12.007>.
- [24] C. Saiprakash, A. Mohapatra, B. Nayak, and S. R. Ghatak, "Analysis of partial shading effect on energy output of different solar PV array configurations," *Materials Today: Proceedings*, vol. 39, pp. 1905–1909, Jan. 2021, <https://doi.org/10.1016/j.matpr.2020.08.307>.
- [25] C. Tubniyom, R. Chatthaworn, A. Suksri, and T. Wongwuttanasatian, "Minimization of losses in solar photovoltaic modules by reconfiguration under various patterns of partial shading," *Energies*, vol. 12, no. 1, Jan. 2019, <https://doi.org/10.3390/EN12010024>.
- [26] V. Balaraju and C. Chengaiah, "A Comprehensive Study on Re-arrangement of Modules Based TCT Configurations of Partial Shaded PV Array with Shade Dispersion Method," *Trends in Renewable Energy*, vol. 6, no. 1, pp. 37–60, Feb. 2020, <https://doi.org/10.17737/tre.2020.6.1.00111>.
- [27] H. Patel and V. Agarwal, "MATLAB-Based Modeling to Study the Effects of Partial Shading on PV Array Characteristics," *IEEE Transactions on Energy Conversion*, vol. 23, no. 1, pp. 302–310, Mar. 2008, <https://doi.org/10.1109/TEC.2007.914308>.
- [28] B. Aljafari, P. R. Satpathy, and S. B. Thanikanti, "Partial shading mitigation in PV arrays through dragonfly algorithm based dynamic reconfiguration," *Energy*, vol. 257, Oct. 2022, Art. no. 124795, <https://doi.org/10.1016/j.energy.2022.124795>.
- [29] P. R. Satpathy, B. Aljafari, and S. B. Thanikanti, "Power losses mitigation through electrical reconfiguration in partial shading prone solar PV arrays," *Optik*, vol. 259, Jun. 2022, Art. new. 168973, <https://doi.org/10.1016/J.IJLEO.2022.168973>.
- [30] E. V. Paraskevadaki and S. A. Papanthassasiou, "Evaluation of MPP Voltage and Power of mc-Si PV Modules in Partial Shading Conditions," *IEEE Transactions on Energy Conversion*, vol. 26, no. 3, pp. 923–932, Sep. 2011, <https://doi.org/10.1109/TEC.2011.2126021>.
- [31] I. Faye, A. Ndiaye, D. Kobor, M. Thiame, C. Sene, and L.-G. Ndiaye, "Evaluation of the impact of partial shading and its transmittance on the performance of crystalline silicon photovoltaic modules," *International Journal of Physical Sciences*, vol. 12, no. 21, pp. 286–294, Nov. 2017, <https://doi.org/10.5897/IJPS2017.4666>.
- [32] S. Rezaazadeh, A. Moradzadeh, K. Pourhossein, B. Mohammadi-Ivatloo, and F. P. García Márquez, "Photovoltaic array reconfiguration under partial shading conditions for maximum power extraction via knight's tour technique," *Journal of Ambient Intelligence and Humanized Computing*, Feb. 2022, <https://doi.org/10.1007/s12652-022-03723-1>.
- [33] S. Daraban, D. Petreus, and C. Morel, "A novel global MPPT based on genetic algorithms for photovoltaic systems under the influence of partial shading," in *IECON 2013 - 39th Annual Conference of the IEEE Industrial Electronics Society*, Vienna, Austria, Aug. 2013, pp. 1490–1495, <https://doi.org/10.1109/IECON.2013.6699353>.
- [34] L. L. Jiang, D. L. Maskell, and J. C. Patra, "A novel ant colony optimization-based maximum power point tracking for photovoltaic systems under partially shaded conditions," *Energy and Buildings*, vol. 58, pp. 227–236, Mar. 2013, <https://doi.org/10.1016/j.enbuild.2012.12.001>.
- [35] A. Fathy and H. Rezk, "A novel methodology for simulating maximum power point trackers using mine blast optimization and teaching learning based optimization algorithms for partially shaded photovoltaic system," *Journal of Renewable and Sustainable Energy*, vol. 8, no. 2, Mar. 2016, Art. no. 023503, <https://doi.org/10.1063/1.4944971>.
- [36] H. Rezk, A. Fathy, and A. Y. Abdelaziz, "A comparison of different global MPPT techniques based on meta-heuristic algorithms for photovoltaic system subjected to partial shading conditions," *Renewable*

- and *Sustainable Energy Reviews*, vol. 74, pp. 377–386, Jul. 2017, <https://doi.org/10.1016/j.rser.2017.02.051>.
- [37] Y. Zhang, J. Su, C. Zhang, Z. Lang, M. Yang, and T. Gu, "Performance estimation of photovoltaic module under partial shading based on explicit analytical model," *Solar Energy*, vol. 224, pp. 327–340, Aug. 2021, <https://doi.org/10.1016/j.solener.2021.06.019>.
- [38] S. Boubaker, S. Kamel, and M. Kchaou, "Prediction of Daily Global Solar Radiation using Resilient-propagation Artificial Neural Network and Historical Data: A Case Study of Hail, Saudi Arabia," *Engineering, Technology & Applied Science Research*, vol. 10, no. 1, pp. 5228–5232, Feb. 2020, <https://doi.org/10.48084/etasr.3278>.
- [39] A. Kajihara and A. T. Harakawa, "Model of photovoltaic cell circuits under partial shading," in *2005 IEEE International Conference on Industrial Technology*, Hong Kong, China, Sep. 2005, pp. 866–870, <https://doi.org/10.1109/ICIT.2005.1600757>.
- [40] M. Z. Shams El-Dein, M. Kazerani, and M. M. A. Salama, "Optimal photovoltaic array reconfiguration to maximize power production under partial shading," in *2012 11th International Conference on Environment and Electrical Engineering*, Venice, Italy, Feb. 2012, pp. 255–260, <https://doi.org/10.1109/EEEIC.2012.6221584>.
- [41] M. G. Villalva, J. R. Gazoli, and E. R. Filho, "Comprehensive Approach to Modeling and Simulation of Photovoltaic Arrays," *IEEE Transactions on Power Electronics*, vol. 24, no. 5, pp. 1198–1208, Feb. 2009, <https://doi.org/10.1109/TPEL.2009.2013862>.
- [42] Y. J. Wang and P. C. Hsu, "An investigation on partial shading of PV modules with different connection configurations of PV cells," *Energy*, vol. 36, no. 5, pp. 3069–3078, 2011, <https://doi.org/10.1016/J.ENERGY.2011.02.052>.

## AUTHORS PROFILE



**Abdullahi A. Masud** received his BE Degree in Electrical Engineering from Ahmadu Bello University (ABU) in 1999. Subsequently, he pursued his Master's degree in the same discipline at ABU and graduated in 2003. He has also obtained a PhD in Electrical Engineering in 2013 from the Glasgow Caledonian University, Scotland, UK. In 2002 he became an assistant lecturer in the Faculty of Engineering at the Ahmadu Bello University, Zaria, Nigeria. In 2013 he joined Jubail Industrial College, Saudi Arabia, and is currently an Associate Professor in the Department of Electrical Engineering. He has several publications in high impact factor journals and conference proceedings in high voltage partial discharge and renewable energy. He is a Chartered Engineer, a Member of the IET, and a registered Engineer (COREN) Nigeria.